

# CONTINUOUS FLOW BEAD-MILLING IMPACT ON SULFUR CURING FOR ADVANCED ELASTOMERIC RUBBER COMPOSITES

MOHAMAD FIRDAUS OMAR<sup>1,2</sup>, FATHILAH ALI<sup>1\*</sup>,  
MOHAMMED SAEDI JAMI<sup>1</sup>, AZLIN SUHAIDA AZMI<sup>1</sup>, FARAH AHMAD<sup>1</sup>,  
MOHD ZAHID MARZUKI<sup>3</sup>, AND JAMAROSLIZA JAMALUDDIN<sup>4</sup>

<sup>1</sup>*Department of Chemical Engineering and Sustainability, Kulliyah of Engineering, International Islamic University Malaysia, P.O. Box 10, 50728 Kuala Lumpur, Malaysia.*

<sup>2</sup>*SC Johnson Asia Pacific Sdn. Bhd., UOA Corporate Tower, The Vertical, 8, Jalan Kerinchi, Bangsar South, 59200 Kuala Lumpur, Malaysia.*

<sup>3</sup>*Faculty of Chemical Engineering, Universiti Teknologi MARA (UiTM) 40450 Shah Alam, Selangor, Malaysia.*

<sup>4</sup>*Department of Chemical Engineering, School of Chemical and Energy Engineering, Universiti Teknologi Malaysia, 81310 Johor Bahru, Johor, Malaysia.*

\*Corresponding author: [fathilah@iium.edu.my](mailto:fathilah@iium.edu.my)

(Received: 7 November 2023; Accepted: 6 October 2024; Published on-line: 15 July 2024)

**ABSTRACT:** As an eco-friendly and technically feasible method for physical modification of materials, bead-milling has been extensively used in many industrial applications ranging from chemicals, nanomaterials, foods, and pharmaceuticals with impacts on particle size, surface morphology, stability, and overall products' performance. Apparently, there have been limited studies conducted on sulfur curative dispersion using this technology, necessitating a thorough investigation of its performance. The objectives of the present study were to explore the influence of the bead-milling process parameters, particularly rotational speed and flow rate, on the sulfur curative dispersion characteristics and to analyze its behavior within the rubber elastomer matrix. Taguchi's L9 orthogonal array experimental design was employed to identify the optimal rotational speed and flow rate of a 60-L bead-milling machine on the sulfur curative dispersion. The stability and morphology of the resulting sulfur curative dispersion were characterized, along with its mechanical properties in rubber elastomers. It was found that higher rotational speed (800 rpm) and lower flow rate (350 L/h) of the bead-milling process resulted in smaller sulfur particle sizes, leading to improved tensile strength of the rubber elastomer. This research may provide valuable insights to determine the ideal bead-milling process for sulfur curative, enhancing the mechanical properties and overall performance of elastomeric rubber composites as well as across various fields.

**ABSTRAK:** Sebagai sebahagian kaedah mesra alam dan secara teknikal dapat mengubah suai bentuk fizikal bahan, mesin pengisaran manik telah digunakan secara meluas dalam kebanyakan aplikasi industri termasuk kimia, nanomaterial, makanan, dan farmaseutikal dengan kesan pada saiz zarah, morfologi permukaan, kestabilan, dan prestasi keseluruhan produk. Namun, terdapat kurang kajian terhadap taburan kuratif sulfur menggunakan teknologi ini, menyebabkan penyelidikan menyeluruh diperlukan bagi menilai prestasinya. Objektif kajian ini adalah bagi mengkaji pengaruh parameter proses pengisaran manik, terutamanya pada kelajuan putaran dan kadar aliran, iaitu terhadap ciri-ciri taburan kuratif sulfur dan mengkaji tindak balasnya pada matriks elastomer getah. Reka bentuk eksperimen Taguchi L9 bersusunan ortogonal telah digunakan bagi mengenal pasti kelajuan putaran dan

kadar aliran optimal mesin pengisaran manik 60 liter terhadap taburan kuratif sulfur. Kestabilan dan morfologi taburan kuratif sulfur yang terhasil telah dicirikan, bersama sifat mekanikal dalam elastomer getah. Dapatan mendapati bahawa proses pengisaran manik pada kelajuan putaran lebih tinggi (800 rpm) dan kadar aliran lebih rendah (350 L/j) menyebabkan saiz zarah sulfur lebih kecil, membawa kepada peningkatan kekuatan regangan elastomer getah. Kajian ini mungkin memberikan pengetahuan penting bagi menentukan proses pengisaran manik yang ideal untuk kuratif sulfur, meningkatkan sifat mekanikal dan prestasi keseluruhan komposit getah elastomerik serta pelbagai bidang lain.

---

**KEYWORDS:** *bead-milling, sulfur, rubber.*

## 1. INTRODUCTION

The bead-milling process has been recognized as an eco-friendly and technically feasible method for the physical modification of materials that can give a mechanochemical effect to the characteristics of a material through friction, collision, impact, and shear from the milling beads and the mill's chamber or container wall. This physical modification is not only able to produce variations of outcome in terms of the particle size, surface properties, and morphology – where the chemical reactions and alteration may impact the structural, physical, and chemical properties – but also in terms of solubility index as well as functional properties such as water absorption, swelling capacity, pasting, and gelation of the milled materials [1–3].

Many researchers reported the use of bead-milling processes as one of the approaches to physically modify their products or materials to achieve the desired characteristics. A study on the effects of multi-wall carbon nanotubes (MWCNTs) and the bead-milling process parameters on aluminum-magnesium (Al-Mg) alloy powder structure proved that increasing time and speed of the bead-milling process leads to the formation of finer particles, which consequently intensifies the plastic deformation and results in a smaller crystallite size. The results indicated that the crystal size was reduced by almost 83%, which consequently improved the distribution of the MWCNTs as well as enhanced their diffusion into the Al-Mg matrix [4]. Other than that, a study on wheat gluten protein's structural and functional properties using bead-mill processing also proved significant outcomes. Those outcomes include breaking of disulfide bonds in gluten, increasing the free sulfhydryl groups, improving the surface hydrophobicity from 940.97 to 1197.50, enhancing the foaming capacity from 8.7 to 31 cm<sup>3</sup>, reducing the particle size from 85.9 to 32.3 μm; and increasing in whiteness from 49.51 to 65.59, indicating the advantage of bead-milling technology in improving the physicochemical properties of wheat gluten that diversifies its application potential [5]. Besides that, another study conducted to produce an ultrafine drug nanocrystal suspension that can pass through 0.22 μm sterilization filters found that finer milling beads, as in 0.1 mm yttrium-stabilized zirconia beads, were the most optimal beads size to mill the AZD4854 drug compound finely at the milling conditions of 2 hours milling time and 700 rpm rotation speed. Plus, the ultrafine drug suspensions were stable, and they did not sediment after several months of refrigeration – making them advantageous in ensuring a homogenous dose in clinical settings without the need for sonication or stirring [6]. Furthermore, the bead-milling method enhances the stability and performance of cesium lead bromide perovskite quantum dots/polymethyl methacrylate (CsPbBr<sub>3</sub> PQDs/PMMA) composites, where the use of the 1.5% CsPbBr<sub>3</sub> PQDs/PMMA composite prepared by the said method not only demonstrated excellent performance with a photoluminescence quantum yield (PLQY) of approximately 78% and high stability, but also exhibited high luminous efficiency in a white light-emitting diode, and its luminescence played a significant role in Rhodamine B (RhB) degradation under visible light [7]. It was highlighted in the paper that the benefits of the bead-milling method include its straightforwardness, being

free from solvent and ligand, being able to operate at low synthesis temperatures, and being easily scalable. These examples of studies show that bead-milling has been used extensively in studies for many potential industrial applications ranging from chemicals, nanomaterials, food processing as well as pharmaceutical drug manufacturing with impacts on particle size, surface morphology, stability, as well as overall performance of the products studied.

Separately, a curing agent, also known as a curative, is a chemical agent used to initiate a chemical reaction, particularly in cross-linking elastomer molecules. When used alongside an accelerator(s) and activator(s) at a significant temperature, the curative forms stable covalent carbon-carbon double bonding. Sulfur is a commonly used curative for rubber elastomers, and it should have a purity of at least 99.5% with very minimal ash content to achieve a maximized curing performance. It can be prepared in a colloid or dispersion state through mixing and/or milling processes, which in turn produces fine sulfur particles that remain suspended (stable) and are suitable for latex compounding in rubber elastomer manufacturing. Remarkably, the solubility of sulfur inside the rubber elastomer system is another critical aspect to look at, where typically, the use of insoluble sulfur is preferred over soluble sulfur to address potential “sulfur blooms” issues in uncured rubber. These blooms can hinder the adhesion of rubber to adjacent layers or substrates, affecting the performance of molded rubber elastomer products. While complete dissolution is usually achieved upon mixing the compound ingredients, unexpected blooms can still occur during actual industrial processing due to the reversion of insoluble sulfur to orthorhombic soluble sulfur before the rubber is cured. Consequently, the sulfur supersaturates the rubber over time, leading to the formation of crystals within the bulk rubber and initiating growth toward the surface [8, 9]. As a result, extensive research has explored methods to enhance the characteristics of sulfur curatives while minimizing blooming events in rubber compounds, which encompass optimizing process parameters such as the use of ball-milling to improve sulfur curative dispersion [10], chemical modification of sulfur for better compatibility with rubber elastomers [11], as well as incorporation of nanoscale additives to enhance mechanical properties [12]. These investigations aim to enhance sulfur's properties and dispersion within rubber, ultimately leading to the development of high-performance elastomeric materials.

Although a lot of studies have been done on different milling parameters over the products' behavior, fewer studies have been done, particularly on sulfur dispersion, and a comprehensive investigation is needed to assess any changes in sulfur properties after bead-milling. The primary objectives of this research are to investigate the influence of continuous flow bead-milling process parameters on the behavior of sulfur curative and its subsequent impact on the performance of elastomeric rubber composites. Specifically, the study aims to explore how varying milling parameters, such as rotational speed and flow rate, affect the dispersion and stability of sulfur curative within the rubber matrix. By understanding these interactions, the research aims to optimize the bead-milling process for sulfur curative, leading to the production of elastomeric articles with enhanced overall performance via characterizations on stability, visual, morphology, and tensile properties by using a Stability Analyzer, a Light Emitting Diode (LED) magnifier lens, Scanning Electron Microscopy / Energy Dispersive X-Ray Analyzer (SEM/EDX), and a Universal Testing Machine (UTM) respectively. Furthermore, the article seeks to contribute valuable insights that can be applied to other industrial applications, promoting the use of bead-milling as an eco-friendly and technically feasible method for enhancing material characteristics in various fields.

## 2. MATERIALS AND METHODS

### 2.1. Chemicals

The main materials used in this project include Hi-Pure Double-Refined sulfur powder supplied by Taiko Group, a surfactant of sodium salt of naphthalene-sulfonic acid from Behn Meyer Group, and deionized water. For the preparation of the rubber elastomer, the high-ammonia natural rubber latex used was obtained from Getahindus Sdn. Bhd. and the compounding ingredients were all industrial grades from Behn Meyer Group, including the high-ammonia natural rubber latex, calcium carbonate, potassium hydroxide, zinc dibutyl-dithiocarbamate, zinc oxide, antioxidant, and coagulant premix with minimum 94% purity each.

### 2.2. Characterizations

To determine the particle size in terms of  $D_{90}$  value of the sulfur curative bead-milled dispersion, a HORIBA Particle Size Analyzer of LA-960V2 model was utilized. Other than that, Total Solids Content (TSC) was calculated to ensure proper control of water loss or excess input. TSC, measured in percentage, was measured as the remaining weight of sample after drying with the aid of an oven at 100 °C, expressed in terms of the original weight of the wet sample as in Eq. 1.

$$TSC \% = \left[ \frac{(\text{weight of dry sample+container}) - (\text{weight of empty container})}{(\text{weight wet sample+container}) - (\text{weight empty container})} \right] \times 100\% \quad (1)$$

The pH value of the sulfur curative dispersion was crucial for its compatibility with rubber as a curing agent, and thus, it should be carefully maintained within the alkaline range. A Brookfield viscometer was utilized together with its RV04 spindle type to assess the dispersion's viscosity.

Furthermore, the stability of selected sulfur dispersion samples after the bead-milling process was analyzed using a multi-sample photo centrifuge – LUMiSizer LS650, providing insights into the dispersion's stability. The properties of the elastomeric rubber samples produced were analyzed in terms of mechanical properties and morphological behavior. A universal testing machine supplied by GT Instruments Sdn. Bhd. (Model: AI-3000) was used to test the tensile strength of the samples, and the samples' thicknesses were measured using a thickness gauge to ensure they were within  $0.06 \pm 0.005$  mm. The morphological behavior of the rubber samples was observed using an LED magnifier lens and SEM/EDX machine, enabling detailed microphotographs to support the understanding of the sulfur curative's behavior within the rubber elastomer matrix.

### 2.3. Process Equipment

The general process started with transporting the raw materials for sulfur dispersion into a 4 MT mixing tank. The tank's mixing time and speed were optimized before the sulfur was continuously pumped into a CDS-60 60-litre continuous large-flow bead-milling machine. The bead-milling machine was equipped with approximately 140 kg and 0.9 mm-sized Yttrium-stabilized Zirconia beads. The parameters studied for this process were rotational speed (motor speed) and flow rate (pump rate).

### 2.4. Preparation of Sulfur Curative

The dispersion of sulfur curative was done by mixing the raw materials for sulfur curative dispersion using the formula provided in Table 1. The mixing speed and time were set at 800

rpm and 30 minutes, respectively. Subsequently, the sulfur curative dispersion was continuously pumped to flow into a CDS-60 60-litre continuous flow bead-milling machine for further processing. The parameters under study for this process were rotational speed and flow rate with respective values and units (Table 2), and the runs were selected using Taguchi's L9 orthogonal array in Table 3 to analyze the different process parameters' outcomes.

## 2.5. Rubber Elastomer Casting

For latex compounding, 4 significant samples of sulfur from the bead-milling process were chosen primarily based on their particle size,  $D_{90}$ . The chemical formulation for compounding was prepared in Table 4, with the dosage calculated in per hundred rubber (phr). The latex compounding process involved mixing the chemicals in a beaker before incorporating them into the raw latex. The compounded latex was then stirred and matured for 36 to 48 hours.

Table 1. Ingredients in preparing sulfur curative dispersion

| Ingredients   | Weight Percentage (%) |
|---|-----------------------|
| Deionized water                                     | 34.0                  |
| Surfactant sodium salt of naphthalene-sulfonic acid | 6.0                   |
| Sulfur curative solids                              | 60.0                  |
| TOTAL   | 100.00                |

Table 2. Control factors with their respective levels for sulfur curative bead-milling

| Factors | Parameter (unit)       | Levels |     |     |
|---------|------------------------|--------|-----|-----|
|         |                        | 1      | 2   | 3   |
| A       | Rotational Speed (rpm) | 800    | 700 | 600 |
| B       | Flow Rate (L/h)        | 750    | 550 | 350 |

Table 3. Taguchi's L9 orthogonal array experimental design on sulfur curative bead-milling

| Run No. | A<br>Rotational Speed | B<br>Flow Rate |
|---------|-----------------------|----------------|
| 1       | Level 1               | Level 1        |
| 2       | Level 1               | Level 2        |
| 3       | Level 1               | Level 3        |
| 4       | Level 1               | Level 1        |
| 5       | Level 2               | Level 1        |
| 6       | Level 2               | Level 2        |
| 7       | Level 3               | Level 1        |
| 8       | Level 3               | Level 2        |
| 9       | Level 3               | Level 3        |

The rubber films were then cast using glaze-coated ceramic plates. The process was initiated by heating the ceramic plates in an oven at 70 °C. The formers were then dipped into a coagulant premix and left to dry in a 60 °C oven. After dipping the formers into the latex compound for 5 to 7 seconds, they were cured in oven at 120 °C for 20 minutes before they were left to cool prior stripping the cast rubber elastomers from the ceramic plates.

Table 4. Formulation of natural rubber latex compound for rubber elastomer making

| Compounding Ingredient       | Dosage (phr) |
|------------------------------|--------------|
| Natural rubber latex         | 100          |
| Calcium carbonate filler     | 30           |
| Potassium hydroxide          | 1.4          |
| Zinc dibutyl-dithiocarbamate | 0.2          |
| Sulfur curative              | 1.2          |
| Zinc oxide                   | 1.0          |
| Antioxidant                  | 0.5          |

### 3. RESULTS AND DISCUSSION

#### 3.1. Curative Properties and Stability Analysis

Table 5 shows the dispersion characteristics of sulfur curatives achieved through varying bead-milling process parameters. The dispersion properties include pH, TSC, viscosity, and particle size. Triplicate samples of sulfur curatives were taken, and their properties recorded for each run and averaged out. The particle size values were assessed further to understand how this property is impacted by the changes in the bead-milling process parameters.

Table 5. Sulfur curative specifications results

| Run No. | Rotational Speed (rpm) | Flow Rate (L/h) | pH  | TSC (%) | Viscosity (cP) | Particle Size, D <sub>90</sub> (µm) |
|---------|------------------------|-----------------|-----|---------|----------------|-------------------------------------|
| 1       | 800                    | 750             | 9.5 | 61.31   | 472            | 7.750                               |
| 2       | 800                    | 550             | 9.5 | 62.99   | 610            | 6.718                               |
| 3       | 800                    | 350             | 9.6 | 61.63   | 598            | 6.154                               |
| 4       | 700                    | 750             | 9.7 | 62.05   | 470            | 8.650                               |
| 5       | 700                    | 550             | 9.9 | 61.84   | 646            | 7.760                               |
| 6       | 700                    | 350             | 9.5 | 62.31   | 616            | 6.820                               |
| 7       | 600                    | 750             | 9.7 | 62.43   | 370            | 9.998                               |
| 8       | 600                    | 550             | 9.7 | 62.69   | 432            | 8.444                               |
| 9       | 600                    | 350             | 9.5 | 61.89   | 518            | 7.214                               |

From Table 5, it can be roughly observed that particle size and viscosity demonstrated variations across the different runs, while pH and TSC were observed to be constant with fewer variations. This variation in particle sizes may be able to influence the resulting dispersion's stability and performance within the rubber matrix. Thus, Fig. 1 was plotted, representing the graph of the effect of particle size on means according to the responses of Taguchi's L9 orthogonal array in Table 6. The calculation and response analysis for the means plot and Signal-to-Noise (S/N) ratio for the particle size in D90 was based on a smaller-is-better analysis for the effects' investigation, which means that the lower or smaller the particle size value, the better the response. Thus, the "mean of means" was plotted in Fig. 1 to signify the trend of the particle size based on the average particle sizes from Table 6.

It can be observed from both the table and figure that the particle size is inversely proportional to the bead mill's rotational speed and directly proportional to the flow rate. Particle size reduction is greatest at higher collision rate of rolling or rotating beads inside the milling chamber, where it is achievable at higher mixing speed and more frequent milling time [13]. Fig. 2, in turn, illustrates particles that are dispersed and then crushed between rolling beads [14].

Intuitively, the bead mill's rotational speed can affect the rate of energy input into the system, having concomitant effects on the process efficiency – where at very low rotational speed, the system would be likely to have very poor mixing in the system, leading to sedimentation of the various materials in the milling chamber that limits total particles milling [15]. The behavior at very high speed (for example, more than 800 rpm in this study) may not be so clear, although it might be expected that the efficiency continues to decrease until there are practical limitations to the increases (such as the material leaving the bead-mill's chamber). Additionally, higher speeds are likely to cause a move away from a stable flow pattern. However, a lower speed is more efficient when considering milling energy. If the control was the total volume of material that achieves the required size reduction in a given period of time, then the effect result may favor higher rotational speeds. For this reason, full-scale plants from this chemical plant use higher rotational speed to enable greater plant throughput, which in turn can increase the overall plant efficiency [15].

In conjunction with this, upon being adsorbed on material surfaces, surfactant molecules provide electrostatic and steric forces to stabilize the particles in the milling media, minimizing the uncontrolled breakdown of particles. Relatively, the sulphonate surfactant used in this study can also aid in lowering the surface energy of the freshly formed fine particles of sulfur dispersion by forming a thin organic layer and introducing long-range capillary forces that lower the energy for crack propagation. The smaller particle size formed at a higher milling rotational speed and slower flow rate is due to the inhibition of the particles from agglomeration the agglomeration will substantially increase particle sizes in the high-energy milling operation employed [16].

Table 6. The particle size of sulfur curative dispersion after bead-milling

| Run No. | Rotational Speed (rpm) | Flow Rate (L/h) | Mean D <sub>90</sub> (µm) | Standard Deviation | S/N Ratio |
|---------|------------------------|-----------------|---------------------------|--------------------|-----------|
| 1       | 800                    | 750             | 7.750                     | 0.2143             | -17.7890  |
| 2       | 800                    | 550             | 6.718                     | 0.1057             | -16.5455  |
| 3       | 800                    | 350             | 6.154                     | 0.0338             | -15.7837  |
| 4       | 700                    | 750             | 8.650                     | 0.1363             | -18.7414  |
| 5       | 700                    | 550             | 7.760                     | 0.1322             | -17.7981  |
| 6       | 700                    | 350             | 6.820                     | 0.0740             | -16.6769  |
| 7       | 600                    | 750             | 9.998                     | 0.1250             | -19.9990  |
| 8       | 600                    | 550             | 8.444                     | 0.0473             | -18.5311  |
| 9       | 600                    | 350             | 7.214                     | 0.0836             | -17.1647  |

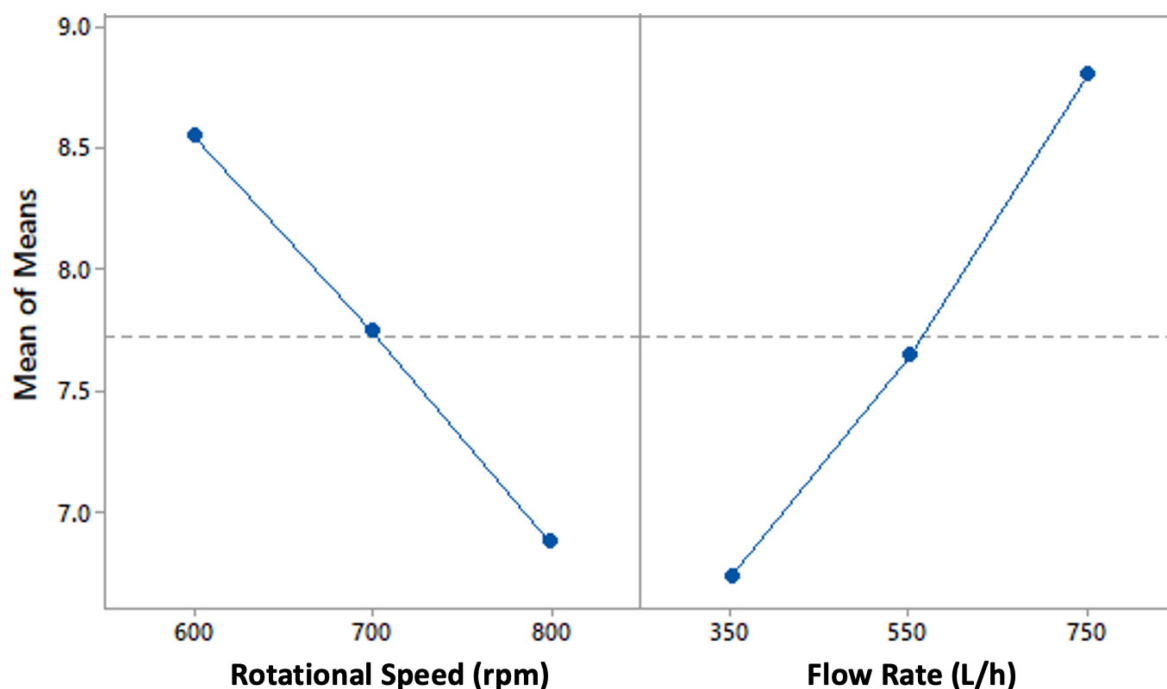


Figure 1. Effect of bead-milling parameters on particles size, D<sub>90</sub> mean of means

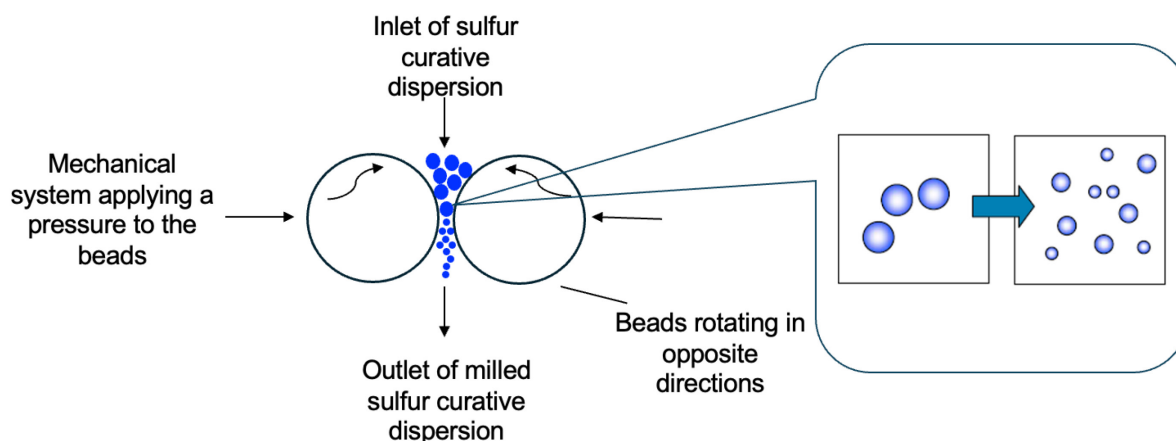


Figure 2. Illustration of particles in between rolling beads in solid particle dispersion by bead-milling

Table 7. ANOVA on sulfur curative dispersion bead-milling particle size

| Source           | DF | Adj SS  | Adj MS  | F-Value | p-Value | Contribution (%)        | Remark      |
|------------------|----|---------|---------|---------|---------|-------------------------|-------------|
| Rotational Speed | 2  | 5.2043  | 2.60216 | 41.56   | 0.002   | 38.81                   | Significant |
| Flow Rate        | 2  | 7.9535  | 3.97675 | 63.52   | 0.001   | 59.32                   | Significant |
| Error            | 4  | 0.2504  | 0.06261 |         |         | 1.87                    |             |
| Total            | 8  | 13.4083 |         |         |         | R <sup>2</sup> = 98.13% |             |

On the other hand, Analysis of Variance (ANOVA) was performed to determine the percent contribution of the operational variables to the response, as in Table 7. The table shows that

the results had been influenced considerably, with the flow rate employed at 59.32 % and rotational speed at 38.81 % influence, respectively. Besides that, the p-values are both less than 0.05 (0.002 and 0.001 for rotational speed and flow rate, respectively), which is close to the significance value (95 % confidence level). At a 95% confidence level, factors having a p-value less than 0.05 are considered significant [17,18], proving these parameters are significant to impact the sulfur's particle size.

The stability analysis for the selected four sulfur curative dispersion samples was conducted using centrifugal separation analysis. Fig. 3 shows the average instability indices of the four different sets of sulfur curative dispersion. Samples A, B, C, and D indicate sulfur curative dispersion after bead-milling, each with different set parameters, which were 800 rpm rotational speed with 350 L/h flow rate, 700 rpm rotational speed with 350 L/h flow rate; 700 rpm rotational speed with 550 L/h flow rate; and 600 rpm rotational speed with 750 L/h flow rate, respectively. The selection of the sulfur was based on the smallest particle size (optimized) and compared with the other three subsequent sulfur sets of various medium to largest size of sulfur. One of them is combined with the lowest viscosity obtained after the bead-milling process.

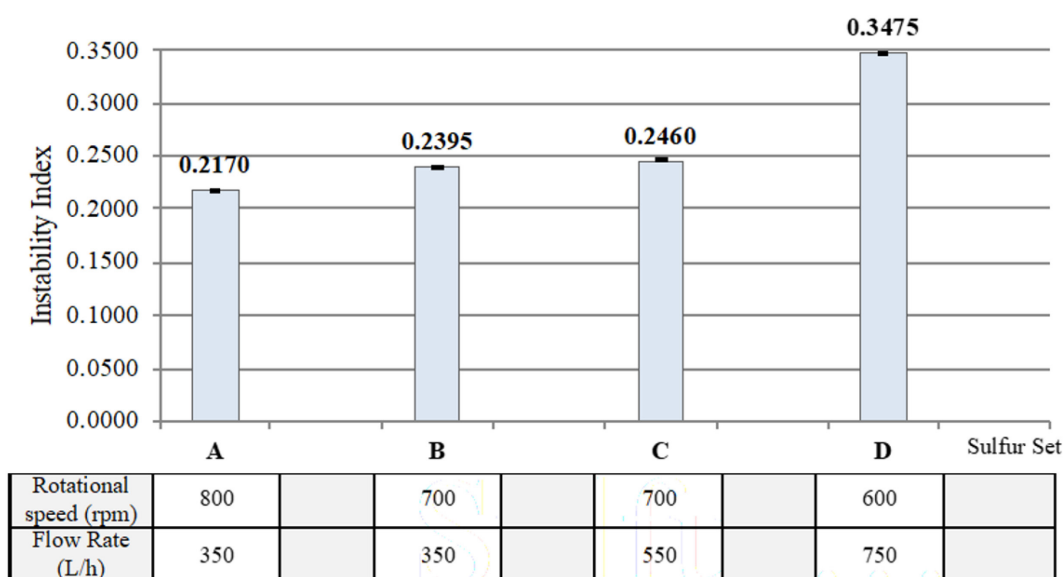


Figure 3. Instability index of different sulfur dispersion bead-milling parameters

It can be observed that the sulfur curative dispersion is most stable for sample A, followed by sample B, C, and D. Briefly, the instability index quantifies the clarification in transmission based on particle size and separation at a given time in the presence of accelerated gravitational force, divided by the maximum clarification possible. The clarification is due to the increase in transmission or decrease in droplet concentration due to the movement of nanodroplets towards the cream layer. It is a dimensionless number between 0 and 1, where 0 indicates no separation or no change in sulfur dispersion's transmission and hence highest stability, and 1 represents complete segregation of phases and hence lowest stability under the centrifugal field. Comparing instability indices of sulfur dispersion under an accelerated gravitational field ultimately aids in a quick comparison of their shelf-life rather than waiting for the separation to occur under normal gravity conditions [19]. Intuitively, more stable sulfur dispersion can be produced at a higher rotational speed that causes more frequent bead collisions in combination with the lower flow rate for sulfur introduction; the sulfur has more time exposed to more bead

collisions, thus altering the sulfur dispersion's chemical properties. Unlike unstable suspension or dispersion, a stable suspension or dispersion will not form aggregates over time. In unstable suspension, particles tend to create particle-particle interactions back, forming aggregates at early stages. Upon late stages, networks of aggregates may form agglomerates that increase particle size and reduce surface area. Networks of agglomerates, in turn, form solid-like gels, which is unfavorable for most applications that use suspensions or dispersions.

### 3.2. Influence on the Resulting Rubber Elastomer

Table 8 shows the rubber elastomer film observation results as seen from the LED magnifier lens while Table 9 shows the microphotographs of the rubber elastomer films under SEM/EDX after they were stored at room temperature for 30 days. From Table 8, obviously, a lot of sulfur crystals/bloom were observed on the rubber film surface for a lower rotational speed of bead-milling of 600 rpm at a higher flow rate of 750 L/h. From the microphotographs and the following spectrum table analysis in Table 9, sulfur can be seen to be one of the dominant elements present on the rubber films (as in column of Spectrum "S"). However, the percentage of presence differs for each different rubber film with different sulfur dispersion produced at designated different bead-milling parameter settings. Set A, with higher rotational speed and lower flow rate of bead-milling, has significantly lower sulfur content on the surface, and Set D, with lower rotational speed and higher flow rate of bead-milling, has higher sulfur content dominance on the rubber film. This analysis supports the observation from the LED magnifier lens results in Table 8.

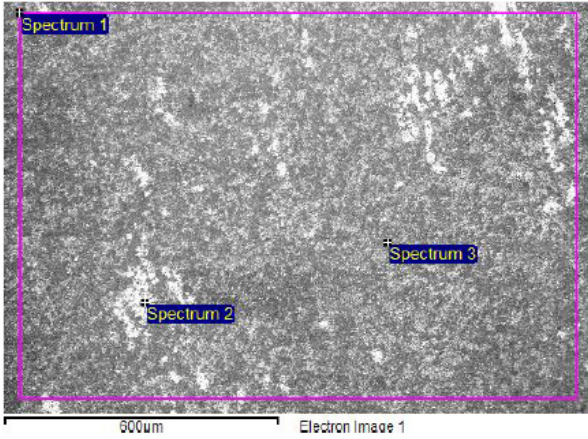
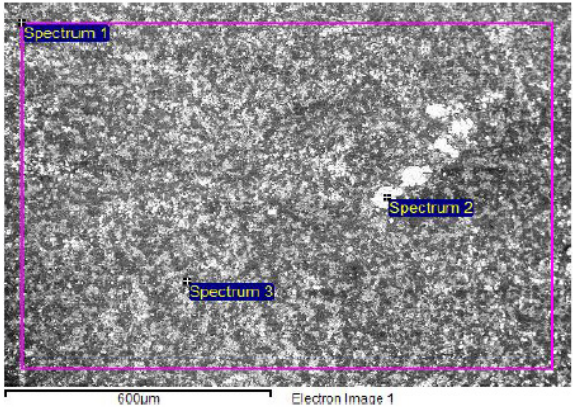
According to the writings by [20,21], insoluble sulfur is usually used rather than soluble sulfur to overcome the "sulfur blooms" issue in unvulcanised rubber. This blooming can minimize the adhesion of rubber to the adjacent layer of rubber or substrate and consequently hinder the performance of the resulting molded rubber articles. Complete dissolution is normally achievable upon mixing the compound ingredients, including insoluble sulfur, because the mixing temperature is high enough to melt sulfur and prevent crystallization. However, when subjected to actual processing in industrial practice, normally unexpected blooms still occur due to the reverting of insoluble sulfur to the orthorhombic soluble sulfur well before the rubber is cured. Eventually, the sulfur supersaturates the rubber when the stock is cooled for a long period of time, and thus, the soluble portion of the sulfur forms crystals within the bulk rubber and initiates growth towards the surface and crystallizes there due to the lack of interference. This might be due to the instability of the sulfur dispersion when processed at this bead-milling parameter setting. From this observation, choosing a less suitable parameter set for sulfur processing could potentially destabilize insoluble sulfur to convert into soluble sulfur that, in turn, migrate to the surface of the rubber to produce blooms.

Fig. 4 illustrates the tensile strength mechanical properties of the cast rubber elastomer films across the four different sulfur curative sets, comparing their respective particle sizes. The mechanical properties underwent testing to assess the mechanical behavior of the rubber elastomer samples according to the ASTM D3578 standard and remarkably passed the minimum requirement of the standard ( $\geq 18$  MPa) [22]. The values for each set remained closely aligned, with slight improvements in tensile strength evident for Set A, which featured the smallest particle size, showing the highest tensile strength value, which apparently contributed to this positive impact.

Table 8. Visual observation of rubber film with different sulfur dispersion bead-milling parameters using an LED magnifier lens

| Sulfur Bead-milling Set   | Pictorial observation;<br>3.0 x magnification  | Visual Observation   |
|---|--|--|
| <b>Set A</b><br>Rotational Speed: 800 rpm<br>Flow Rate: 350 L/h |    | Less to zero sulfur crystals / bloom observed on the rubber film           |
| <b>Set B</b><br>Rotational Speed: 700 rpm<br>Flow Rate: 350 L/h |   | Less to zero sulfur crystals / bloom observed on the rubber film           |
| <b>Set C</b><br>Rotational Speed: 700 rpm<br>Flow Rate: 550 L/h |  | Less tiny particles of sulfur crystals / bloom observed on the rubber film |
| <b>Set D</b><br>Rotational Speed: 600 rpm<br>Flow Rate: 750 L/h |  | A lot of sulfur crystals / bloom observed on the rubber film               |

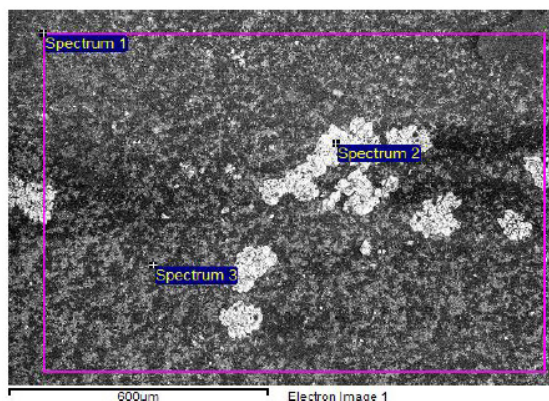
Table 9. SEM/EDX elemental analysis on rubber film of different sulfur dispersion bead-milling parameters

| Sulfur Bead-Milling Set  | Sulfur-dispersed rubber film with area of sulfur crystals/bloom (Magnification: 200X) |       |      |       |      |             |             |      |       |
|--|---|-------|------|-------|------|-------------|-------------|------|-------|
| <p><b>Set A</b></p> <p>Rotational Speed:<br/>800 rpm</p> <p>Flow Rate: 350 L/h</p> |     |       |      |       |      |             |             |      |       |
|  | Spectrum  | C     | N    | O     | Mg   | Al          | S           | Cl   | Ca    |
|  | Spectrum 1  | 62.71 | 0.00 | 23.76 | 0.17 | 0.24        | <b>3.08</b> | 0.34 | 9.71  |
|  | Spectrum 2  | 58.96 | 0.00 | 23.27 | 0.19 | 0.26        | <b>7.25</b> | 0.30 | 9.77  |
|  | Spectrum 3  | 59.24 | 0.00 | 24.33 | 0.20 | 0.29        | <b>3.04</b> | 0.40 | 12.50 |
| Standard Deviation   | 1.71  | 0.00  | 0.43 | 0.01  | 0.02 | <b>1.98</b> | 0.04        | 1.30 |       |
| <p><b>Set B</b></p> <p>Rotational Speed: 700 rpm</p> <p>Flow Rate: 350 L/h</p>     |   |       |      |       |      |             |             |      |       |
|  | Spectrum  | C     | N    | O     | Mg   | Al          | S           | Cl   | Ca    |
|  | Spectrum 1  | 65.61 | 0.00 | 21.95 | 0.15 | 0.19        | <b>4.10</b> | 0.21 | 7.79  |
|  | Spectrum 2  | 54.17 | 0.00 | 27.58 | 0.18 | 0.24        | <b>7.96</b> | 0.34 | 9.22  |
|  | Spectrum 3  | 62.47 | 0.00 | 22.71 | 0.14 | 0.20        | <b>3.15</b> | 0.25 | 11.09 |
| Standard Deviation   | 4.83  | 0.00  | 2.49 | 0.02  | 0.02 | <b>2.08</b> | 0.05        | 1.35 |       |

**Set C**

Rotational Speed: 700 rpm

Flow Rate: 550 L/h

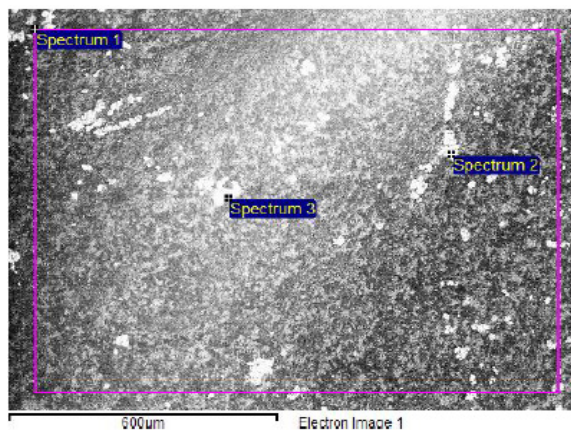


| Spectrum           | C     | N    | O     | Mg   | Al   | S            | Cl   | Ca    |
|--------------------|-------|------|-------|------|------|--------------|------|-------|
| Spectrum 1         | 64.67 | 0.00 | 21.90 | 0.14 | 0.19 | <b>4.76</b>  | 0.36 | 7.98  |
| Spectrum 2         | 56.84 | 0.00 | 6.68  | 0.07 | 0.00 | <b>33.78</b> | 0.14 | 2.49  |
| Spectrum 3         | 58.37 | 0.00 | 29.32 | 0.25 | 0.03 | <b>1.64</b>  | 0.28 | 10.10 |
| Standard Deviation | 3.39  | 0.00 | 9.42  | 0.07 | 0.08 | <b>14.47</b> | 0.09 | 3.21  |

**Set D**

Rotational Speed: 600 rpm

Flow Rate: 750 L/h



| Spectrum           | C     | N    | O     | Mg   | Al   | S            | Cl   | Ca    |
|--------------------|-------|------|-------|------|------|--------------|------|-------|
| Spectrum 1         | 62.09 | 0.00 | 23.45 | 0.24 | 0.07 | <b>3.36</b>  | 0.33 | 10.46 |
| Spectrum 2         | 58.83 | 0.00 | 10.38 | 0.09 | 0.04 | <b>26.80</b> | 0.00 | 3.85  |
| Spectrum 3         | 58.16 | 0.00 | 7.01  | 0.03 | 0.10 | <b>31.74</b> | 0.15 | 2.81  |
| Standard Deviation | 1.72  | 0.00 | 7.09  | 0.09 | 0.02 | <b>12.38</b> | 0.13 | 3.39  |

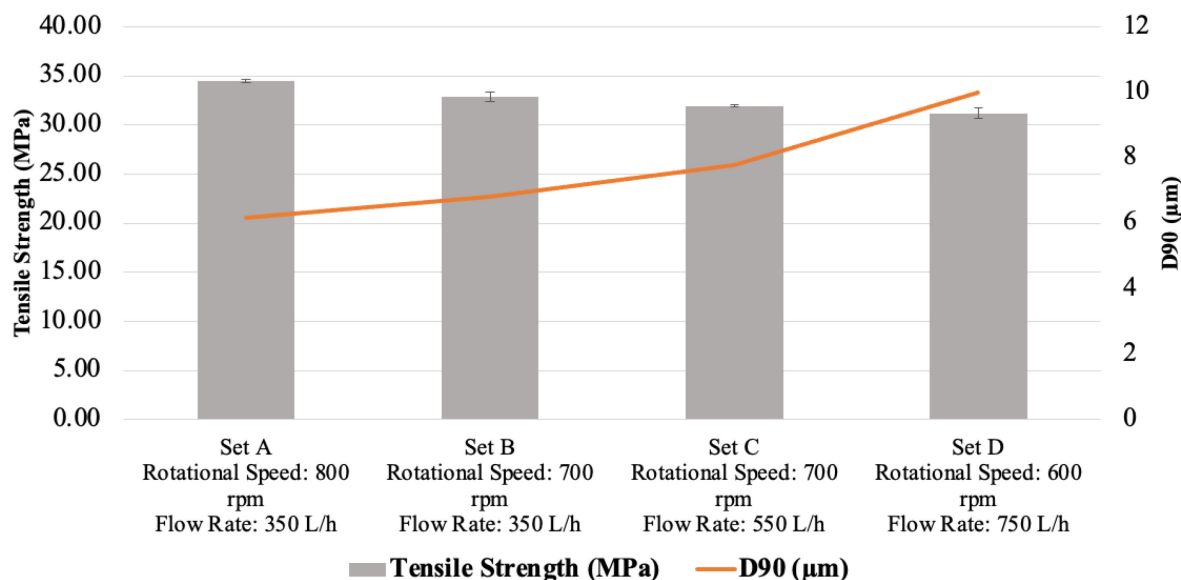


Figure 4. Tensile strength of cast rubber elastomer films with different bead-milled sulfur curative.

## 4. CONCLUSION

In conclusion, this study investigated the impact of bead-milling process parameters, namely rotational speed and flow rate, on sulfur curative dispersion and its subsequent effects on rubber elastomer properties. The findings revealed that higher rotational speed (800 rpm) and lower flow rate (350 L/h) resulted in smaller sulfur dispersion particle sizes, which slightly improved the tensile strength of rubber elastomers and significantly reduced the formation of sulfur crystals. This bead-milling process parameter setting also improved sulfur dispersion stability from the lowest instability index result. The visual observations and morphology analysis confirmed the influence of bead-milling parameters on the presence of sulfur crystals on rubber film surfaces. Overall, the research highlights the potential for eco-friendly processes such as bead-milling to optimize overall properties and material characteristics of dispersion products in various industrial applications, particularly in elastomeric rubber composites.

## ACKNOWLEDGEMENT

Mohamad Firdaus Omar would like to extend his appreciation to the Department of Chemical Engineering and Sustainability in IIUM that made this work possible. The authors gratefully acknowledge the financial support of research funding from Universiti Teknologi Malaysia, UTM Fundamental Research vote no. 22H56.

## REFERENCES

- [1] Tan, X, Zhang, B, Chen, L, Li, X, Li, L, Xie, F. (2015) Effect of Planetary Ball-Milling on Multi-Scale Structures and Pasting Properties of Waxy and High-Amylose Cornstarches. *Innovative Food Science & Emerging Technologies*, 30: 198–207. <https://doi.org/10.1016/j.ifset.2015.03.013>.
- [2] Páramo-Calderón, DE, Vázquez-León, LA, Palma-Rodríguez, HM, Utrilla-Coello, RG, Vargas-Torres, A, Meza-Nieto, MA, Romero-Cortes, T, Aparicio-Saguilán, A. (2023) Effect of High-Energy Mechanical Milling on the Physicochemical and Rheological Properties of Chayotextle (*Sechium Edule Sw.*) Starch. *Food Chemistry*, 427: 136720. <https://doi.org/10.1016/j.foodchem.2023.136720>.

- [3] Bangar, SP, Singh, A, Ashogbon, AO, Bobade, H. (2023) Ball-Milling: A Sustainable and Green Approach for Starch Modification. *International Journal of Biological Macromolecules*, 237: 124069. <https://doi.org/10.1016/j.ijbiomac.2023.124069>.
- [4] Ahmadian, H, Sallakhniknezhad, R, Zhou, T, Kiahosseini, SR. (2022) Mechanical Properties of Al-Mg/MWCNT Nanocomposite Powder Produced under Different Parameters of Ball Milling Process. *Diamond and Related Materials*, 121: 108755. <https://doi.org/10.1016/j.diamond.2021.108755>.
- [5] Liu, Z, Zheng, Z, Zhu, G, Luo, S, Zhang, D, Liu, F, Shen, Y. (2021) Modification of the Structural and Functional Properties of Wheat Gluten Protein Using a Planetary Ball Mill. *Food Chemistry*, 363: 130251. <https://doi.org/10.1016/j.foodchem.2021.130251>.
- [6] Carling, C-J, Pekkari, A. (2023) Bead Milled Drug Nanocrystal Suspensions Fine Enough to Pass through 0.22 Mm Sterilization Filters. <https://doi.org/https://example.net>.
- [7] Liu, W, Xie, H, Guo, X, Wang, K, Yang, C, Wang, N, Ge, C. (2023) Luminescence, Stability, and Applications of CsPbBr<sub>3</sub> Quantum Dot/Polymethyl Methacrylate Composites Prepared by a Solvent- and Ligand-Free Ball Milling Method. *Optical Materials*, 136: 113398. <https://doi.org/10.1016/j.optmat.2022.113398>.
- [8] Motavalizadehkakhky, A, Shahrampour, H. (2018) Determination of the Most Efficient Form of Sulfur for Use as a Natural Rubber Curing Agent by Comparison of Physical and Thermal Attributes of Cured Rubber. *Petroleum Chemistry*, 58: 89–93. <https://doi.org/10.1134/S0965544118010048>.
- [9] Shahrampour, H, Motavalizadehkakhky, A. (2017) The Effects of Sulfur Curing Systems (Insoluble-Rhombic) on Physical and Thermal Properties of the Matrix Polymeric of Styrene Butadiene Rubber. *Petroleum Chemistry*, 57: 700–704. <https://doi.org/10.1134/S0965544117080138>.
- [10] Pangamol, P. (2016) Use of By-Product Sulfur from Petroleum Refinery as Vulcanizing Agent in Natural Rubber. *Chiang Mai J. Sci.*, 43: 569–576. <http://epg.science.cmu.ac.th/ejournal/>.
- [11] Zheng, L, Jerrams, S, Xu, Z, Zhang, L, Liu, L, Wen, S. (2020) Enhanced Gas Barrier Properties of Graphene Oxide/Rubber Composites with Strong Interfaces Constructed by Graphene Oxide and Sulfur. *Chemical Engineering Journal*, 383: 123100. <https://doi.org/10.1016/j.cej.2019.123100>.
- [12] Duan, X, Tao, R, Chen, Y, Zhang, Z, Zhao, G, Liu, Y, Cheng, S. (2022) Improved Mechanical, Thermal Conductivity and Low Heat Build-up Properties of Natural Rubber Composites with Nano-Sulfur Modified Graphene Oxide/Silicon Carbide. *Ceramics International*, 48: 22053–22063. <https://doi.org/10.1016/j.ceramint.2022.04.196>.
- [13] Sopicka-Lizer, M. (2010) High-Energy Ball Milling. Woodhead Publishing Limited. <https://doi.org/10.1533/9781845699444>.
- [14] Flach, F, Konnerth, C, Peppersack, C, Schmidt, J, Damm, C, Breitung-Faes, S, Peukert, W, Kwade, A. (2016) Impact of Formulation and Operating Parameters on Particle Size and Grinding Media Wear in Wet Media Milling of Organic Compounds – A Case Study for Pyrene. *Advanced Powder Technology*, 27: 2507–2519. <https://doi.org/10.1016/j.appt.2016.09.026>.
- [15] Tamblyn, RJ. (2009) Analysis of Energy Requirements in Stirred Media Mills.
- [16] Ullah, M, Ali, Md, Hamid, S. (2014) Structure-Controlled Nanomaterial Synthesis Using Surfactant-Assisted Ball Milling- A Review. *Current Nanoscience*, 10: 344–354. <https://doi.org/10.2174/15734137113096660114>.
- [17] Sudheer, M, Prabhu, R, Raju, K, Bhat, T. (2013) Modeling and Analysis for Wear Performance in Dry Sliding of Epoxy/Glass/PTW Composites Using Full Factorial Techniques. *ISRN Tribology*, 2013: 1–11. <https://doi.org/10.5402/2013/624813>.

- [18] Achuthamenon Sylajakumari, P, Ramakrishnasamy, R, Palaniappan, G. (2018) Taguchi Grey Relational Analysis for Multi-Response Optimization of Wear in Co-Continuous Composite. *Materials*, 11: 1743. <https://doi.org/10.3390/ma11091743>.
- [19] Yerramilli, M, Ghosh, S. (2017) Long-Term Stability of Sodium Caseinate-Stabilized Nanoemulsions. *Journal of Food Science and Technology*, 54: 82–92. <https://doi.org/10.1007/s13197-016-2438-y>.
- [20] Aziz, Y, Hepburn, C. (1979) Problems of Bloom Experienced When Insoluble Sulphur Is Used in Natural Rubber. *Journal of the Rubber Research Institute of Malaysia*, 2: 57–67.
- [21] Jurkowski, B, Jurkowska, B. (1998) On the Mechanism of Sulfur Behavior in Rubber Compounds. *Journal of Macromolecular Science, Part B*, 37: 135–142. <https://doi.org/10.1080/00222349808220461>.
- [22] Ab Rahman, MF, Norfaizal, NS, Azura, AR. (2019) The Influence of Sago Starch Dispersion on Mechanical Properties of Biodegradable Natural Rubber Latex Films. *Materials Today: Proceedings*, 17: 1040–1046. <https://doi.org/10.1016/j.matpr.2019.06.507>.